

Supplementary Information

Integrated Cobalt Disulfide (CoS_2) Co-catalytic Passivation Layer on Silicon Microwires for Photoelectrochemical Hydrogen Evolution

Chih-Jung Chen,^a Po-Tzu Chen,^b Mrinmoyee Basu,^a Kai-Chih Yang,^b Ying-Rui Lu,^{cd} Chung-Li Dong,^c Chong-Geng Ma,^e Chin-Chang Shen,^f Shu-Fen Hu^{*b} and Ru-Shi Liu^{*ag}

^a Department of Chemistry, National Taiwan University, Taipei 10617, Taiwan.

^b Department of Physics, National Taiwan Normal University, Taipei 11677, Taiwan.

^c National Synchrotron Radiation Research Center, Hsinchu 30076, Taiwan.

^d Program for Science and Technology of Accelerator Light Source, National Chiao Tung University, Hsinchu 30010, Taiwan.

^e College of Sciences, Chongqing University of Posts and Telecommunications, Chongqing 400065, China.

^f Institute of Nuclear Energy Research, Atomic Energy Council, Taoyuan 32546, Taiwan.

^g Department of Mechanical Engineering and Graduate Institute of Manufacturing Technology, National Taipei University of Technology, Taipei 10608, Taiwan.

Corresponding authors: E-mail: sfhu.hu@ntnu.edu.tw; Fax: +886-2-29326408; Tel.: +886-2-77346079; and E-mail: rsliu@ntu.edu.tw;

Fax: +886-2-33668671; Tel.: +886-2-33661169

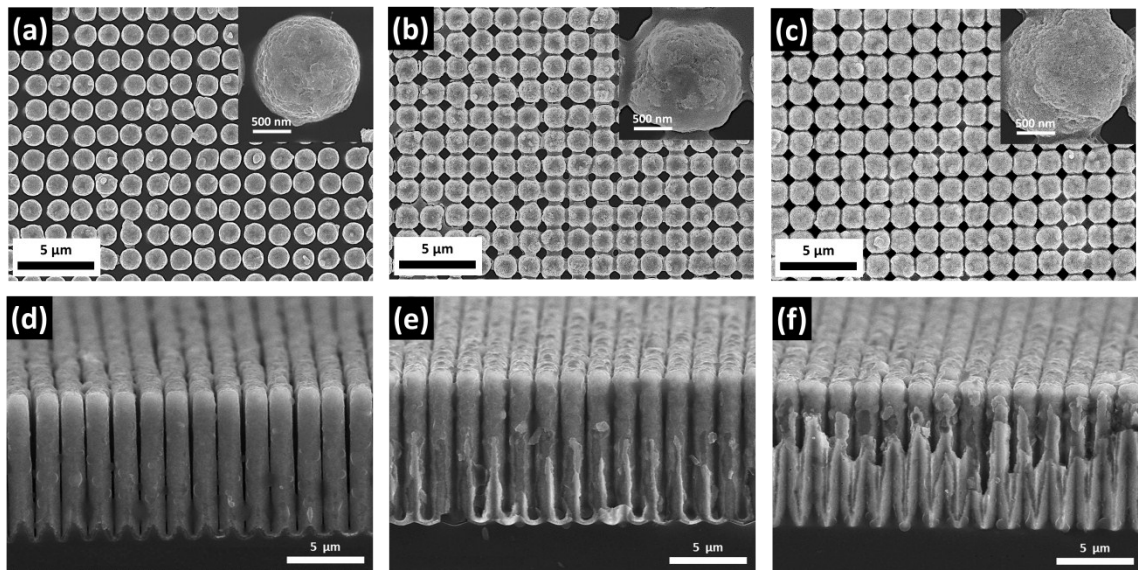


Fig. S1 (a–c) Top view and (d–f) cross-sectional SEM images of $\text{CoS}_2\text{-Si-200}$, $\text{CoS}_2\text{-Si-280}$, and $\text{CoS}_2\text{-Si-310}$ microwire arrays.

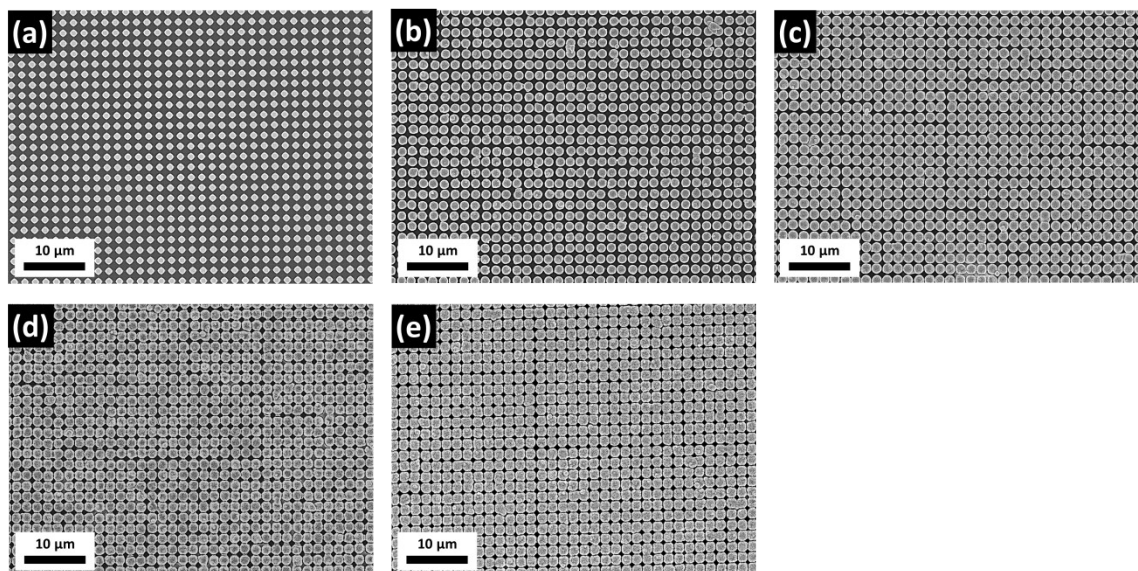


Fig. S2 Low-magnification top-view SEM images of (a) bare Si, (b) $\text{CoS}_2\text{-Si-200}$, (c) $\text{CoS}_2\text{-Si-250}$, (d) $\text{CoS}_2\text{-Si-280}$, and (e) $\text{CoS}_2\text{-Si-310}$ microwire arrays.

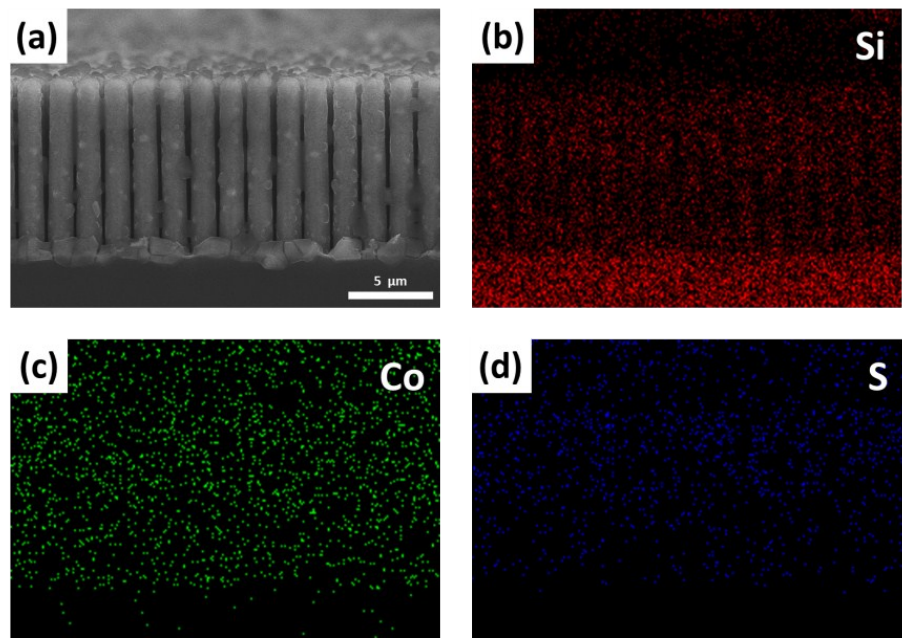


Fig. S3 (a) Cross-sectional SEM images of CoS₂-Si-250 electrode and its elemental mapping of (b) Si, (c) Co, and (d) S.

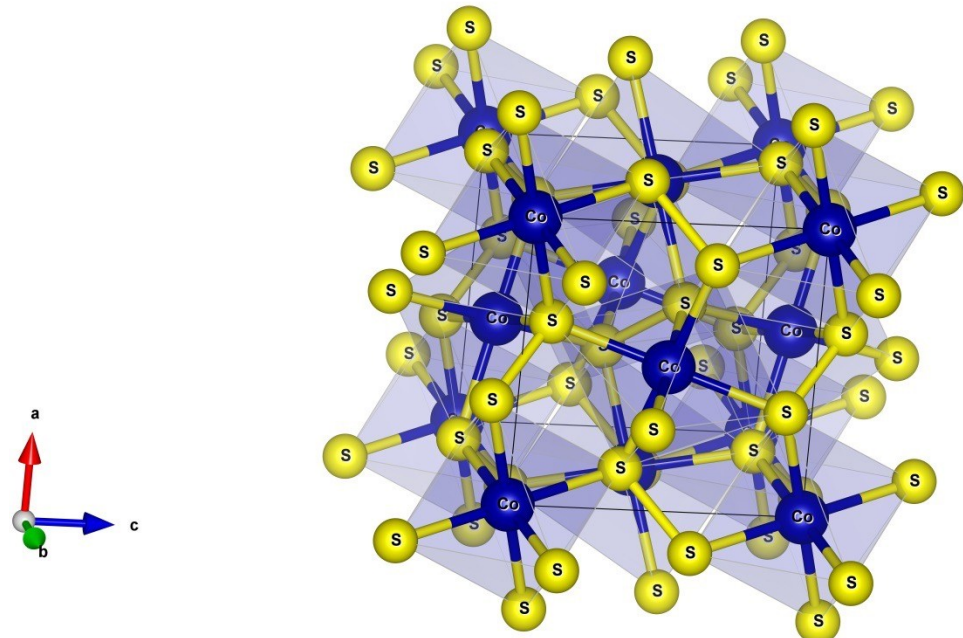


Fig. S4 Schematic illustration of the crystal structures for CoS₂.

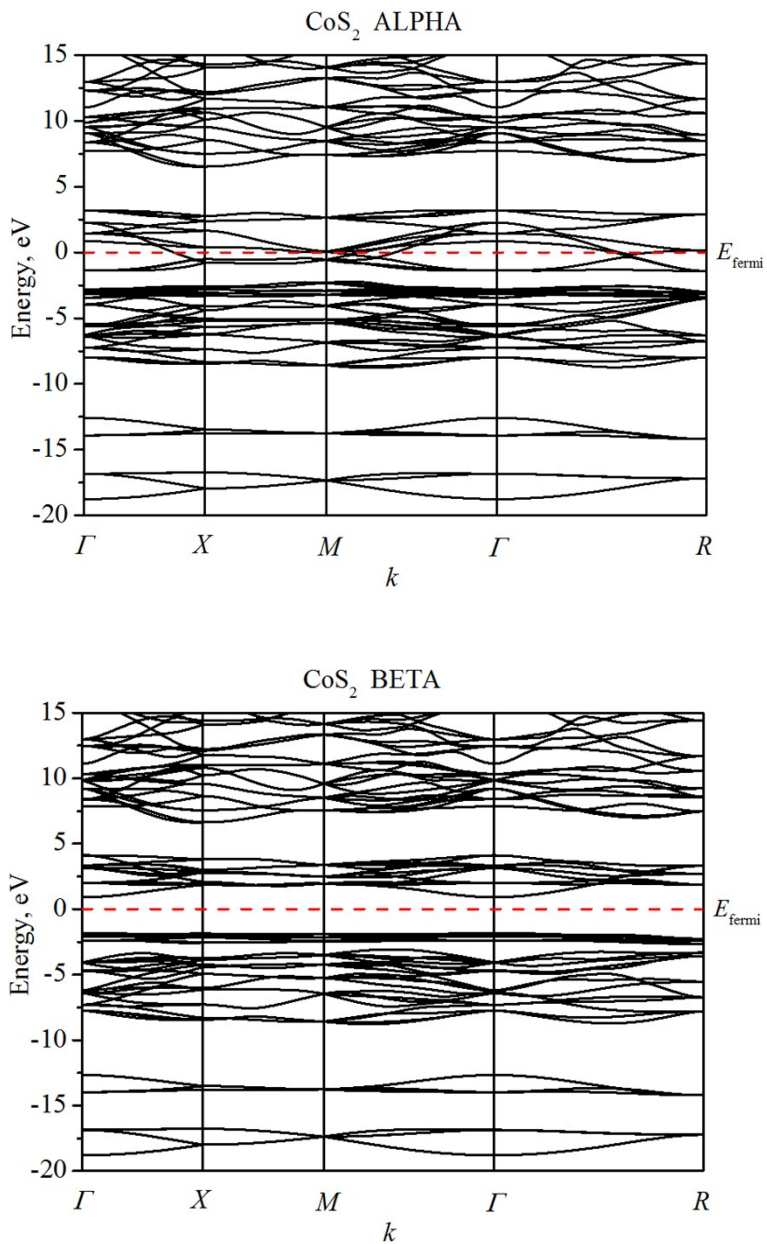


Fig. S5 The red horizontal dashed line denotes the Fermi level position, and the letters Γ , X , M , and R represent the high-symmetry k points: $(0,0,0)$, $(0,1/2,0)$, $(1/2,1/2,0)$, and $(1/2,1/2,1/2)$, respectively.

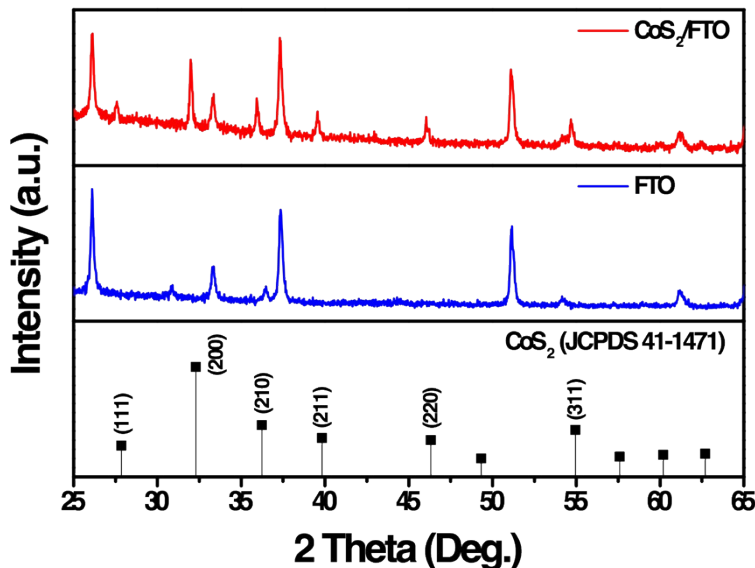


Fig. S6 XRD spectra of CoS_2/FTO electrode and FTO substrate. All diffraction peaks match well with the standard pattern of pyrite phase CoS_2 (JCPDS No. 41-1471).

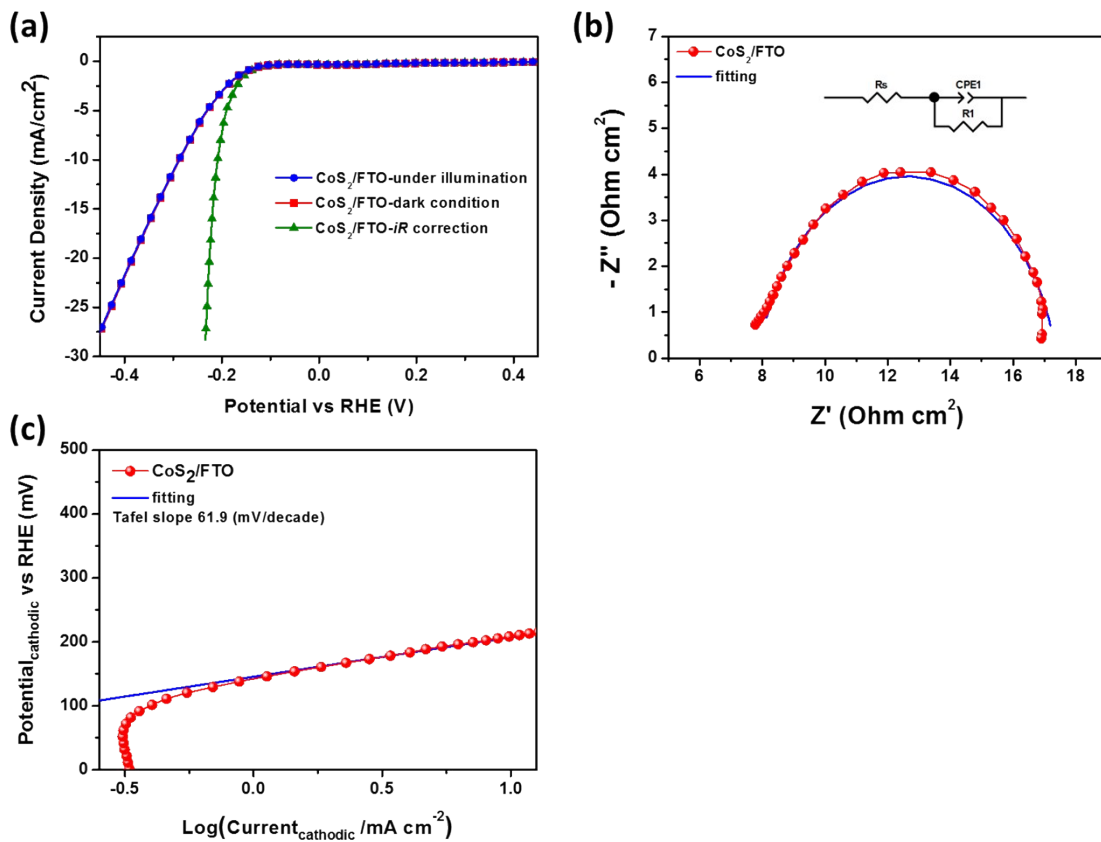


Fig. S7 (a) Linear sweep voltammograms, (b) electrochemical impedance spectroscopy, and (c) Tafel plot of CoS_2/FTO electrode.

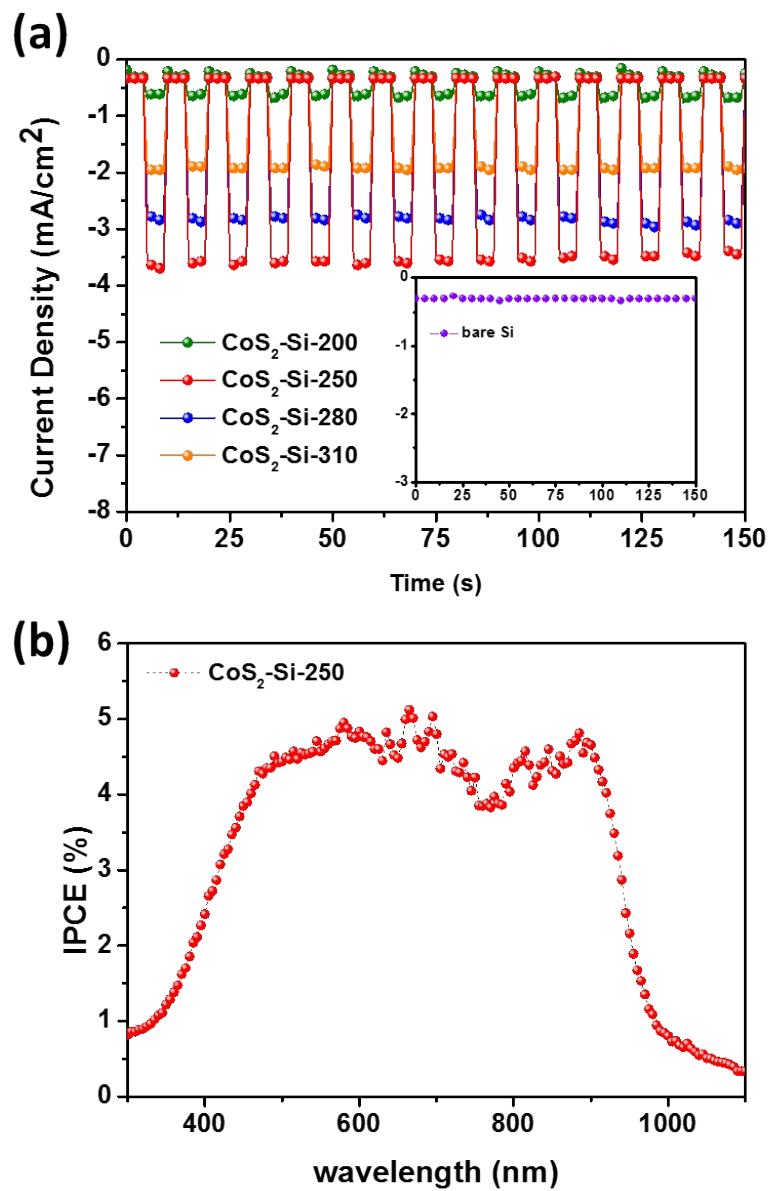


Fig. S8 (a) Transient photocurrent density of CoS₂-Si electrodes with various CoS₂ thicknesses at 0 V.
(b) IPCE of CoS₂-Si-250 electrode under different wavelengths of illumination at 0 V.

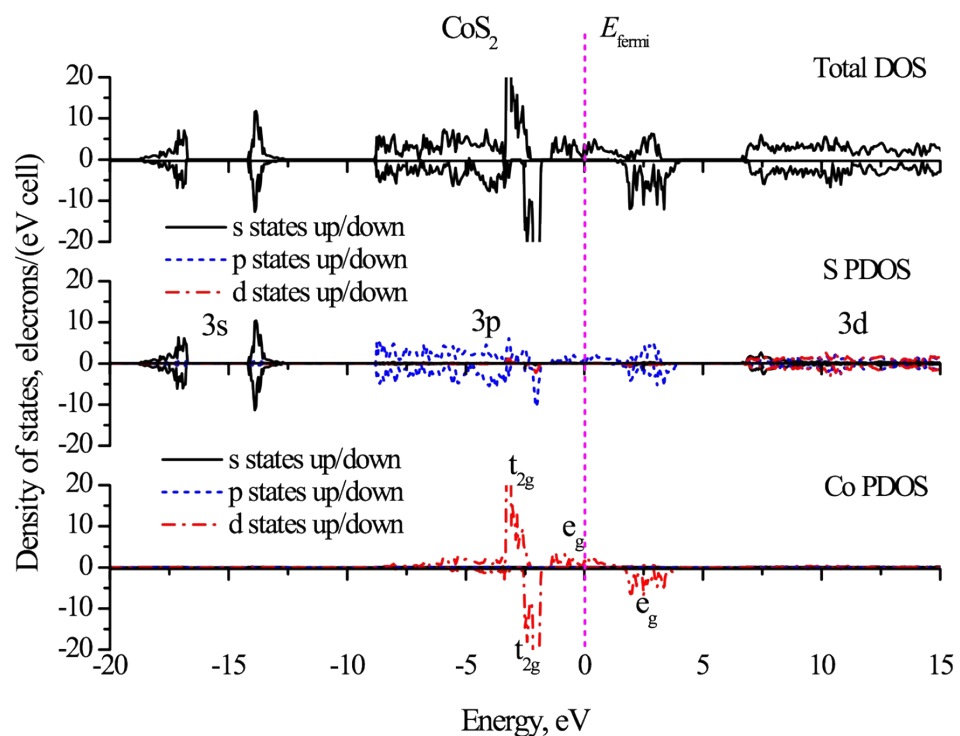


Fig. S9 Calculated PDOS/DOS diagrams for CoS_2 . The purple vertical dashed line denotes the Fermi level position.

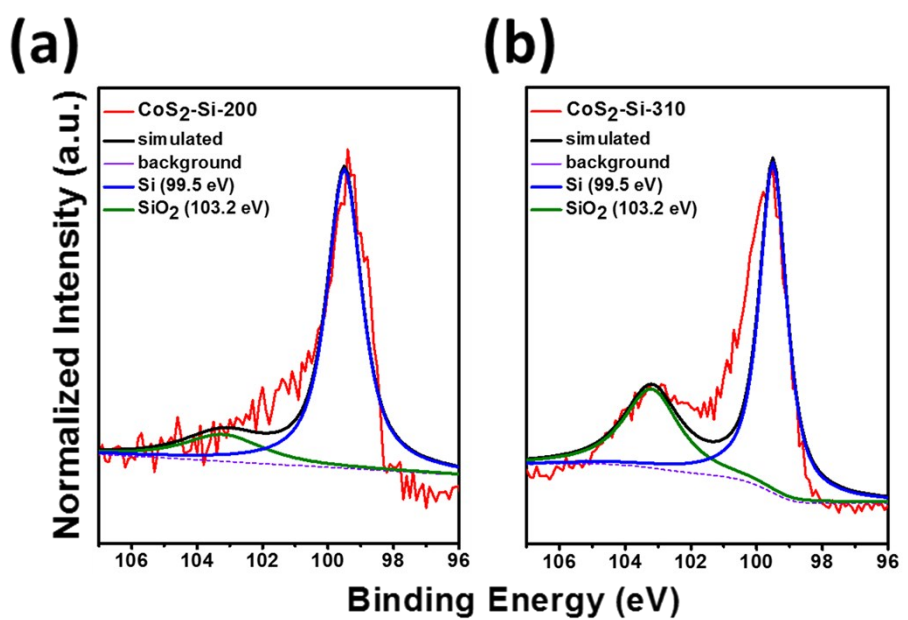


Fig. S10 High-resolution Si 2p spectra of (a) CoS₂-Si-200 and (b) CoS₂-Si-310 electrodes with different coordination conditions.

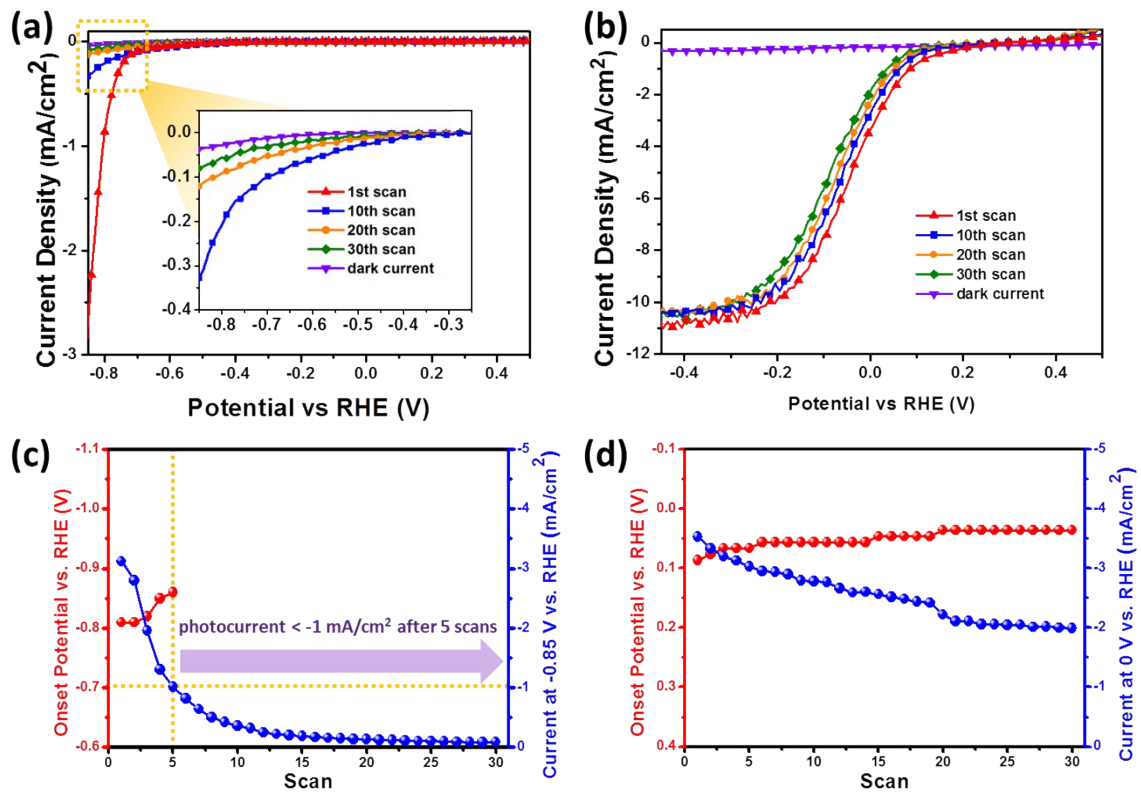


Fig. S11 Linear sweep voltammograms of (a) bare Si and (b) Pt-Si electrodes scanned for 30 times. Onset potential and photocurrent of (c) bare Si and (d) Pt-Si electrodes versus scan times.

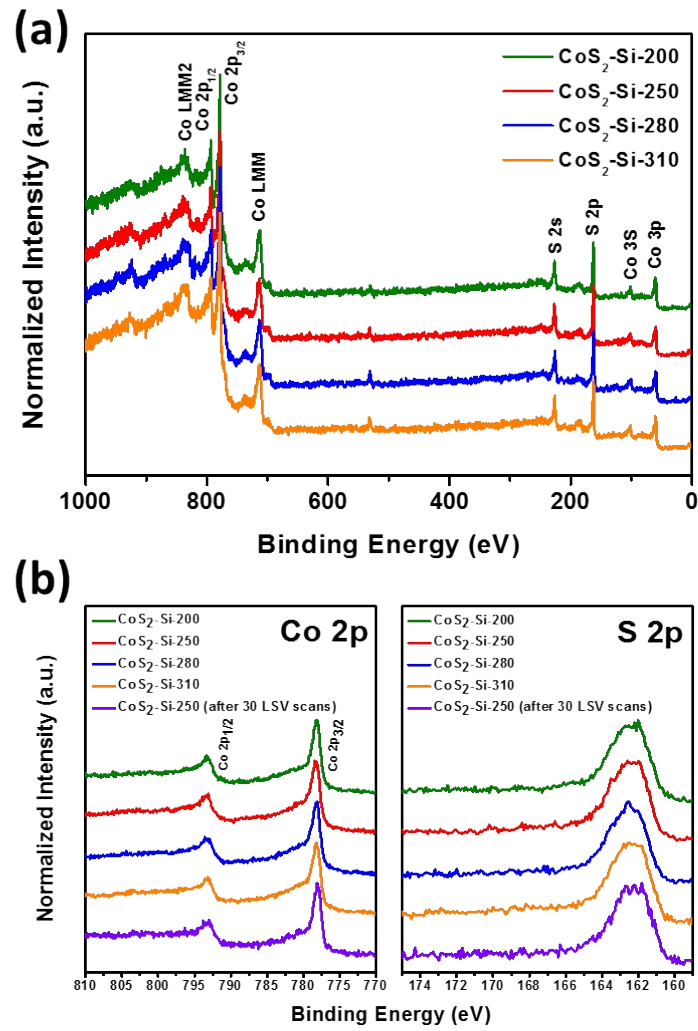


Fig. S12 (a) XPS spectra and (b) high-resolution Co 2p and S 2p XPS spectra of $\text{CoS}_2\text{-Si}$ electrodes with various CoS_2 thicknesses.

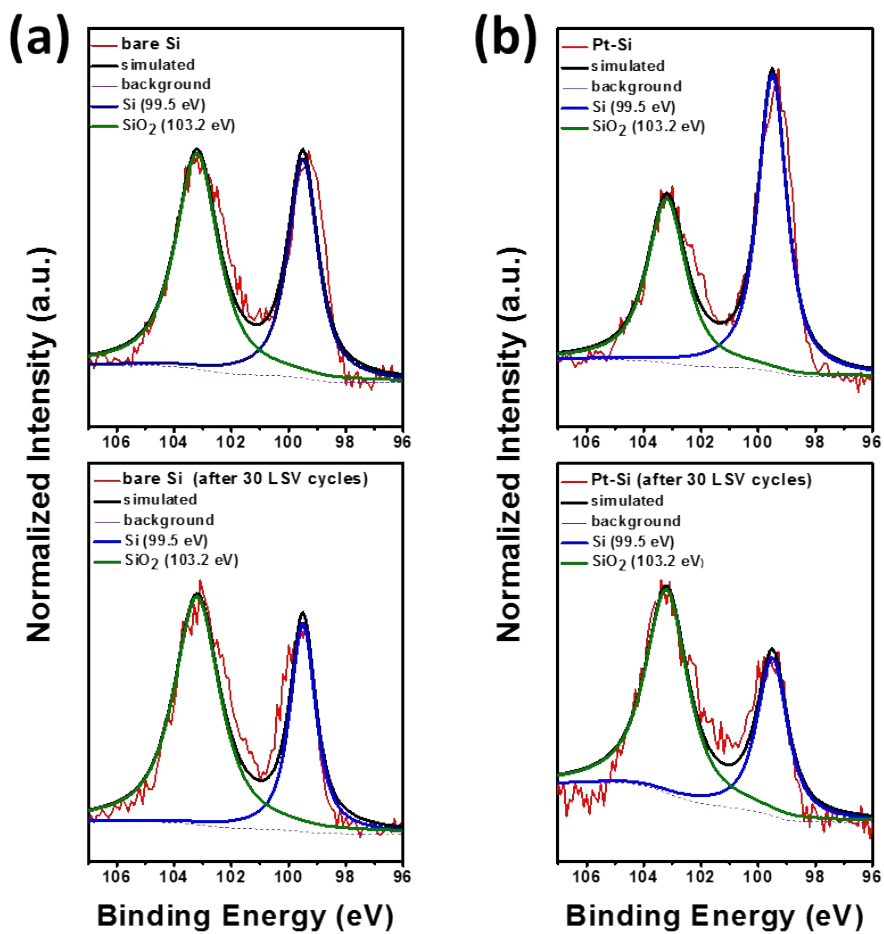


Fig. S13 High-resolution Si 2p spectra of the (a) as-prepared Si electrode and Si electrode after 30 LSV scans, and (b) as-prepared Pt-Si electrode and Pt-Si electrode after 30 LSV scans with different coordination conditions.

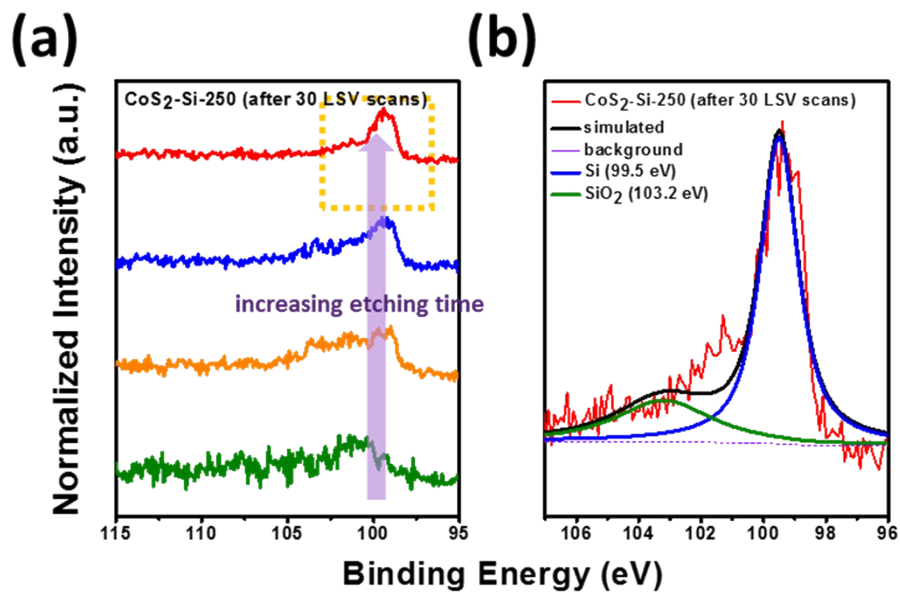


Fig. S14 High-resolution Si 2p spectra of Co₃S₂-Si-250 electrode after 30 LSV scans (b) with increasing Ar ion etching time and (c) different coordination conditions.

Table. S1 Summary of structural and electronic data for CoS₂.

| | CoS ₂ | |
|------------------------------------|-------------------|---------------------------------------|
| | Exp. ^a | Calc. |
| <i>a</i> , Å | 5.5385 | 5.5286 |
| <i>b</i> , Å | 5.5385 | 5.5286 |
| <i>c</i> , Å | 5.5385 | 5.5286 |
| $\alpha=\beta=\gamma$, ° | 90 | 90 |
| Co | 0 | 0 |
| | 0 | 0 |
| | 0 | 0 |
| <i>X</i> | 0.38988 | 0.38811 |
| | 0.38988 | 0.38811 |
| | 0.38988 | 0.38811 |
| <i>R</i> (Co-X), Å | 2.3252 | 2.3172 |
| <i>R</i> (X-X), Å | 2.1128 | 2.1428 |
| <i>Q</i> (Co ²⁺), e | - | 1.094 |
| <i>Q</i> (X), e | - | -0.547 |
| μ (Co ²⁺), μ_B | 0.85 ^b | 1.117 (~1 ^c) |
| μ (X), μ_B | | -0.058(~0 ^c) |
| <i>E</i> _g , eV | | 2.7261($\Gamma \rightarrow \Gamma$) |

Notes: Coordinates of the crystallographic positions (in units of the lattice constants, (x, y, z) from top to bottom) of all ions and the Co-X and X-X chemical bond lengths (*R*) are also given. The electronic data contain the effective Mulliken charge (*Q*) and magnetic moment (μ) of individual ion, as well as the band gap (*E*_g) for beta electrons.

^a Ref. [E. Nowack, D. Schwarzenbach, T. Hahn, Acta Crystallogr., Sect. B: Struct. Sci. 47 (1991) 650]; ^b Ref. [V.N. Antonov, O.V. Andryushchenko, A.P. Shpak, A.N. Yaresko, O. Jepsen, Phys. Rev. B 78 (2008) 094409]; ^cOther calculation result [S. Saha, M. De Raychaudhury, T. Saha-Dasgupta, Phys. Rev. B 77 (2008) 155428.]